

The Role of the Orbitofrontal Cortex in Integral Learning of a 2-Dimensional
Auditory Task

Ruthie Poizner

A Thesis in
The Department of
Psychology

Presented in Partial Fulfillment of the
Requirements for the Degree of Master of Arts
(Psychology) at Concordia University
Montreal, Quebec, Canada

January 2026

© Ruthie Poizner, 2026

Concordia University
School of Graduate Studies

This is to certify that the thesis

Prepared by: Ruthie Poizner

Entitled: The role of the orbitofrontal cortex in integral learning of a 2-dimensional auditory task

and submitted in partial fulfillment of the requirements for the degree of

Master of Arts (Psychology)

complies with the regulations of the University and meets the accepted standards with respect to originality and quality.

Signed by the final Examining Committee:

_____ Chair
Dr. Karen Li

_____ Examiner
Dr. Mihaela Iordanova

_____ Examiner
Dr. Guillem Esber

_____ Supervisor
Dr. Matthew Gardner

Approved by _____
Dr. Karen Li

_____ 2026

_____ *Dr. Pascale Sicotte (Dean of Faculty)*

Abstract

The Role of the Orbitofrontal Cortex in Integral Learning of a 2-Dimensional Auditory Task

Ruthie Poizner

This experiment investigates the role of the orbitofrontal cortex (OFC) in facilitating integral representation of an auditory space. To test rats' ability to learn holistic stimulus dimensions, we trained 20 rats on a Pavlovian task in which 2 sets of auditory cues were configured to represent a 2-dimensional space. The stimuli consisted of 12 distinct tone frequencies and 12 distinct clicker frequencies, which were combined for 144 compound auditory stimuli. 2 of the auditory compound cues were paired with a saccharin reward. We sought to determine whether temporary DREADD-induced inactivation of the OFC across the learning phase of the task would impair learning between the compound stimuli and saccharin. We injected AAV8-CaMKIIa-hM4Di-mCherry (n=11) or AAV8-CaMKIIa-mCherry (n=9) into the OFC prior to the experiment. To learn the stimulus set, rats were exposed to 'random walk' paths through the auditory space, such that they would listen to a progression of compound cues in which each transition consisted of an incremental change in frequency in one of the auditory dimensions. To assess the role of the OFC in learning these compound cues, rats received injections of a DREADD agonist (Agonist 21) or saline throughout the first 16 days of the 34-day experiment. Learning was assessed through reward anticipation and performance on 2 extinction tests (days 17 and 34). OFC-inactivation inhibited the ability of rats to respond in anticipation of the reward based on the particular compound cue configurations, indicating that OFC is required for integral learning in a reward setting.

Acknowledgements

I would like to thank Dr. Matthew Gardner for his support and mentorship throughout this process. His kindness, creativity, and passion for research have inspired me since our first meeting. I have benefitted greatly from working with an involved supervisor who made time for me to discuss our research and anything else.

Thank you to my defense committee, Dr. Mihaela Iordanova, Dr. Guillem Esber, and Dr. Karen Li, for their guidance, review, and feedback.

I would also like to extend my gratitude to Pablo Turrent who helped train me, provided continuous support throughout my experiments, and allowed me to cite his research in this thesis. Further, I want to thank Nuria Larochele for her collaboration on our longest running experiment, Thomas Leir for his friendship and encouragement, and all the members of Dr. Gardner's Lab: Christopher Chacon, Joseph Harb, Toni Kach, Lauren Natovitch, Maryam Ratemi, Elizabeth Rye, Nicholas Vanlianz, and Susana Wang.

Contribution of Authors

This experiment was developed and funded by Dr. Matthew Gardner and Ruthie Poizner. The data from Figures 2 through 4 was collected by Pablo Turrent. The remaining data was collected by Ruthie Poizner. This thesis was written by Ruthie Poizner. All tasks were conducted under the supervision of Matthew Gardner.

Table of Contents

List of Figures	vii
List of Tables	viii
Introduction	1
Integral Learning	1
Multidimensional Stimulus Sets.....	4
Cognitive Maps	6
Localization and the Orbitofrontal Cortex	9
Specialized Cells	13
Methods	14
Subjects	14
Surgical Procedure and Apparatus	15
Behavioural Apparatus	18
Behavioural Paradigm	20
Behavioural Procedure	22
Statistical Analysis	24
Results	24
Discussion	34
Conclusion	40
References	42
Appendix	47

List of Figures

Figure 1: Graph depicting aggregate response percentage by proximity to a rewarded cue.

Figure 2: Diagrams of the cue map exemplifying random walk trajectory, reward zone and complementary zone locations, and distance between pixels in the matrix

Figure 3: Thermal maps depicting aggregate response volume across days from a previous cue map experiment

Figure 4: Bar graph of a previous cue map experiment comparing response slopes at the reward zones and complementary zones

Figure 5: Analysis of response slope in relation to number of pixels away from the reward zones and complementary zones

Figure 6: Bar graph comparing response slopes at the reward zones and complementary zones on the second extinction test

Figure 7: Thermal maps comparing aggregate response volume across days between experimental groups

Figure 8: Slopes comparing responding between reward zones and complementary zones

Figure 9: Between-group comparison of the change in response at reward zones

List of Tables

Table 1: Analysis of variance comparing response slope at reward zones and complementary zones on day 32

Table 2: Analysis of variance results for responding by distance from reward zones

Table 3: Repeated measures analysis of variance by zone type across all days

Table 4: Repeated measures analysis of variance by zone type on day 17

Table 5: Repeated measures analysis of variance by zone type on day 34

Table 6: Analysis of variance results across all trials except extinction tests

Table 7: Analysis of variance results for days 1-16

Table 8: Analysis of variance results for days 18-33

Table 9: Analysis of variance by sex across all trials

Introduction

Cognitive maps refer to individuals' internal models of their environments and the relevant dimensions. While this process has since been studied in a variety of species, the term cognitive map was first formalized by Edward Tolman in his 1948 paper on rats. Over multiple trials, Tolman watched rats navigate mazes in increasingly intuitive ways. He theorized that rats create mental field maps of their environments, and that they can use this information to infer the location of a reward even if they have not previously explored that area. Tolman and his successors observed that cognitive mapping may apply to both physical and abstract spaces (Tolman, 1948; Qiu et al., 2024).

Our experiment investigates the neural and cognitive mechanisms by which rats learn an abstract space. We argue that in order to create a holistic cognitive map, individuals must first learn stimulus dimensions as interdependent (referred to as integral learning). Since the orbitofrontal cortex (OFC) is implicated in the creation of cognitive maps, we hypothesize that the OFC is required to learn compound stimuli as integral dimensions.

Integral Learning

In multidimensional stimulus sets, dimensions may interact to produce the impression of a combined, or integral, stimulus (Garner, 1976; Wagemans et al., 2012). For instance, the Garner paradigm presents subjects with a 2-dimensional stimulus, in which each dimension consists of 2 levels. These levels combine to create four stimuli. In a simplified case of the Garner filtering task, subjects are presented with a colour grid in which squares vary by hue (either blue or purple) and brightness (either light or dark). These dimensions are combined to create four different colour shades: light blue, dark blue, light purple, and dark purple. The stimulus features (i.e. colour shade) of each square are perceived holistically and cannot be

separately analyzed, meaning these dimensions would be categorized as integral (Burns, 2016; Blunden et al., 2015; Smith & Kemler, 1978; Wagemans et al., 2012). Conversely, separable dimensions refer to dimensions that are perceived and analyzed independently. For example, the colour and the shape of an object may be separately attended to and therefore constitute separable stimulus dimensions (Tversky & Gati, 1982).

Integral and separable stimulus sets primarily differ on metrics of similarity scaling, whereby subjects are prompted to rate the similarity between multidimensional stimuli across one or more dimensions, and reaction time (RT) (Garner, 1976; Shepard, 1991; Kato & Okada, 2011). Dimensional integrality is defined by its association with redundancy gain, interference in selective attention tasks, and the use of Euclidean metrics (Garner & Felfoldy, 1970; Garner, 1976; Shepard, 1991). An integral dimension may only exist in relation to a specified level on the other dimension; for instance, as per the filtering task example, a square must be classified not only by its placement on the hue axis but also by its placement on the brightness axis. Conversely, behavioural metrics, such as RT, to separable dimensions are not facilitated by dimensional correlation, and orthogonal dimensions can yield selective attention. Similarity scaling of separable dimensions is generally characterized by a city block metric, in which measurement is divided into separate computations that are then added together (Garner, 1976; Shepard, 1991).

According to Shepard's city block combination rule (1964), dissimilarity between 2 stimuli yields the sum of the dissimilarities between said stimuli on each independent dimension. Since separable dimensions are not processed holistically, they must be broken down by features. Addition of dissimilarities between each dimension (namely, dimensions that yield different

metrics) cannot be blended. Consequently, subjects must analyze the dissimilarities between the dimensions before totaling the result (Blough, 1991).

The application of Euclidean versus city block metrics may extend beyond measurements of physical distance. Psychophysics research argues that individuals may rely on distance measurements to compare the abstract features of stimuli or stimulus dimensions. Further, the type of measurement used generally reflects the degree of stimulus integrality. In 1938, Richardson found evidence that subjects could construct abstract Euclidean colour-spaces based on similarity between the colours. Later, in 1945, Householder and Landahl outlined a mathematical equation describing how people discriminate between distinct stimuli, using city block metrics to compare perceptual differences across dimensions (Householder & Landahl, 1945; Shepard, 1991).

It is worth noting that the use of Euclidean or city block metrics are not necessarily mutually exclusive, and that judgment generally falls somewhere in between. Most researchers argue that pure integrality is approached but never fully achieved, and that dimensional integrality and separability should thus be considered as continuous rather than discrete classifications (Shepard, 1991; Wood, 1974). Data from concept learning research suggests a spectrum of dimensions, ranging from clearly separable to more unitary (Garner, 1976). Furthermore, the impact of integrality on learning varies case by case. Processes such as dimensional filtering and the integration of information may be affected differently depending on the features of the dimensions (Shepard, 1991), which do not always lend themselves to discrete categorization. Stimulus dimensions may be ambiguous in definition (Burns & Shepp, 1988; Cheng & Pachella, 1984), and most research suggests that a dichotomous distinction between integral and separable learning does not capture the full complexity of these processes. For

example, Wood's 1974 study on speech discrimination presented subjects with 3 types of stimulus dimension configurations: a combination of an auditory and a phonetic dimension, a combination of 2 auditory dimensions, and a combination of 2 phonetic dimensions. When combining auditory and phonetic dimensions, he found that the ability to filter irrelevant variation depended on the placement of the variation; namely, subjects were better able to filter variation on the phonetic dimension than they were the auditory one. This suggests that selective attention may be applied asymmetrically. This asymmetry may be a form of perceptual scaffolding, whereby the processing of phonetic stimuli builds upon the processing of auditory stimuli. Wood argued that performance of this task therefore draws on multiple perceptual processes.

Multidimensional Stimulus Sets

As Shepard argued in his paper on a unified theory of generalization (1987), the ability to recognize stimuli that yield the same or similar outcomes is a heuristic. Generalization arises not from an inability to distinguish between stimuli, but rather from the cognitively efficient tendency to identify patterns in the environment and use this information to predict outcomes. Integral dimensions may be viewed as dimensions whose possible outcomes are positively correlated, whereas separable dimensions are unlikely to yield similar outcomes (Shepard, 1991).

Generalization strategies may be divided into 2 categories: configural, which is analogous to integral learning, and elemental, which is analogous to separable learning. The former strategy refers to an averaging effect in which outcomes are a product of their stimulus configurations (Soto, Gershman, & Niv, 2014). Stimulus dimensions are combined in association with the outcome, meaning the configuration is considered holistically when making predictions (Goldfarb et al., 2021). The latter strategy, elemental generalization, represents a summation

effect in which the associative strength is equal to the strength of the elements' algebraic sum (Blough, 1975; Rescorla & Wagner, 1972; Soto, Gershman, & Niv, 2014). When the combined associative strength of a stimulus is high, so is the decremental effect of introducing a nonreinforced stimulus (Rescorla & Wagner, 1972). In elemental learning, individuals generally use each separate cue or stimulus dimension to predict outcomes (Goldfarb et al., 2021).

According to Pearce, generalization is dictated by configural similarities between stimulus sets. Configural learning is generally thought to occur when stimuli are similar, as similar stimuli tend to be predictive of similar outcomes. In contrast, elemental learning is generally thought to occur when stimuli are dissimilar, such as learning between modalities. While most data supports this similarity hypothesis, it is worth noting that there is evidence that stimulus similarity is not necessary for compound generalization (Pearce, 1987; Pearce, 2002; Soto, Gershman, & Niv, 2014).

Both humans and animals rely on generalization processes to adapt within our ever-changing, highly sophisticated environments. Experimental paradigms, which may only outline a few stimuli of interest, do not encapsulate the complexity of reality (Soto et al., 2014). The multidimensional nature of the real world necessitates selective attention, as individuals must navigate complex environments in a cognitively efficient way. Learning requires generalization of past experiences to adapt to new ones. This includes the ability to ignore irrelevant cues, and form hierarchical associations based on context to regulate cue-elicited behaviour (Niv et al., 2015; Peterson et al., 2024). It is hypothesized that the brain therefore reduces dimensionality to only those that are relevant for tasks such as reward prediction, and that this reduced representation is updated through constant trial and error. Neural research suggests the existence of a bilateral attentional network localized in the intraparietal sulcus, the precuneus, and the

dorsolateral prefrontal cortex. This network is thought to interact with the basal ganglia to facilitate learning and the filtering/selection of relevant dimensions (Niv et al., 2015).

Cognitive Maps

Cognitive maps may describe mental representations of physical landscapes, such as city blocks, or abstract landscapes (Qiu et al., 2024), such as the experimental design used in this thesis. This process is thought to facilitate flexible cognition and behaviour, allowing humans and animals to efficiently navigate an ever-changing environment (Behrens et al., 2018; Park et al., 2020). Whether processing a physical or abstract landscape, cognitive maps allow individuals to make inferences about new situations based on previously learned information. These maps can help guide behaviour in novel situations, appraise new stimuli, and aid in the efficiency and effectiveness of learning. Extrapolating from previously learned information helps individuals fill in the gaps and predict outcomes when dealing with unknown variables (Behrens et al., 2018; Park et al., 2020). Using cognitive maps, individuals can speculate about the outcomes of certain actions and predict whether these actions will yield reward or punishment (Wilson et al., 2014). Furthermore, understanding cognitive maps may shed light on other psychological processes such as schema formation, generalization, planning, prediction, and decision making (Behrens et al., 2018; Park et al., 2020). The ability to accurately map relations between abstract and concrete stimuli is a hallmark of higher order cognition, and likely essential for model-based decision making. This process relies on an individual's ability to piece together information from long-term memory, forming a detailed, integrated model of the world around them (Park et al., 2020). Individuals can integrate information from across modalities to form a holistic, cohesive cognitive map (Behrens et al., 2018).

Mental models of the environment play a vital role in spatial navigation and can help individuals determine new routes and shortcuts (Park et al., 2020). Evidence suggests that subjects are better able to navigate both cognitive and motor tasks if they have experienced similar situations prior (Zhou et al., 2021). Tolman himself found that over multiple trials, rats discovered increasingly efficient and enterprising ways to obtain the reward. This effect was observed despite changes to the maze's landscape (1948). Harry Harlow's primates showed similar effects. When performing a discrimination task, the subjects displayed an ability to generalize skills from previous trials to discriminate between novel stimuli. The process of "learning to learn" describes how cognitive maps acquired from previous trials scaffolds future learning (Behrens et al., 2018).

Like Harlow's, Tolman's findings revealed a level of abstract cognition not inherent to stimulus-response learning. He argued that with learning, rats develop a mental map that enables dynamic perspective. While cognitive maps may range in complexity, the process of learning a map requires more autonomy than forming a stimulus-response association. Tolman proposed that maps necessitate cognitive manipulation and attention to the relationship between stimuli and the environment (1948).

In addition to learning the structure of the environment, Tolman's rats also showed evidence of latent learning. In unrewarded trials, rats spent more time wandering through the maze. In later trials, when the reward was introduced, rats displayed sudden efficiency in navigating the maze, yielding fewer errors. This suggests that rats can draw upon a previously learned map when it is contextually beneficial. Further experiments reaffirm that rats can develop wider cognitive maps than what is specifically trained (Tolman, 1948). These latent states may be comprised of unobservable information, and can be created when little data is

available regarding the outcome of a situation. Creating latent maps enables individuals to strategize different outcomes in the absence of extensive sensory information (Behrens et al., 2018).

This process may be understood through the principle of generalization. In this instance, learning the structure of the physical and psychological environment allows animals to generalize information between similar scenarios that yield the same outcomes (Shepard, 1987). Recognizing common structures between situations expedites learning and enables cognitive adaptability in otherwise uncharted territory (Zhou et al., 2021). Individuals are unlikely to experience wholly identical situations, and some degree of generalization between contexts is therefore inherent to all cognition (Shepard, 1987).

Research has explored the effect of intermittent reinforcement on gradients of generalization. This gradient, which refers to the correlation between conditioned responding to a new stimulus and the similarity between the new and conditioned stimulus, was observed in both humans (Shepard, 1987) and animals (Guttman & Kalish, 1956). This should lead to a generalization decrement: a decrease in conditioned responding as the stimulus features decrease in similarity from the target. Similar findings were observed in Pavlovian tasks. Specifically, dogs who were conditioned to respond to the sound of a bell or whistle exhibited generalization to other sounds but responded especially strongly to those with similar auditory features. While this phenomenon has been observed in multiple animals, gradients of generalization differ between species. Interstimulus generalization may decay at different rates depending on the animal, as well as the sensory features of the conditioned and unconditioned stimuli (Shepard, 1987). These findings indicate the brain's ability to abstract data from its sensory input, integrating physical and psychological information to create a flexible representation of the

environment (Behrens et al., 2018). The ability to extrapolate outcomes from available information is foundational to the creation of a cognitive map, as it allows individuals to orient themselves within a dynamic landscape.

In addition to animal models, neural network data can provide valuable insight into the brain. While it is sometimes argued that higher order cognitive mapping and inferencing is unique to living things (Behrens et al., 2018; Park et al., 2020), artificial intelligence models reveal interesting findings about learning and prediction. Research suggests that even simple information can provide neural networks with the basis for comprehensive structural representations. Like rodents, artificial intelligence can use latent knowledge of a 2-dimensional structure to better predict upcoming sensory events. Both rodents and neural networks are apparently able to spatially reorient within a model (Behrens et al., 2018). The ability to abstract likely scenarios from limited sensory information is an invaluable heuristic. Imagining every possible outcome in a situation is costly, if not impossible. Conversely, inferential planning enables individuals to generalize between similar scenarios to infer probable outcomes, remaining adaptable without wasting mental resources (Behrens et al., 2018).

Localization and the Orbitofrontal Cortex

Although cognitive maps have been studied for the better part of a century, the specific mechanisms underlying this process remain somewhat obscure (Park et al., 2020; Zhou et al., 2021). The OFC, located in the neocortex, has long been an area of interest with regards to cognitive mapping. Research suggests that the OFC is instrumental in the creation, manipulation, and consolidation of these maps. The OFC may play a role in updating existing maps by integrating information from new stimuli and long-term memory, as well as encoding imagined trajectories within the model (Behrens et al., 2018; Gardner & Schoenbaum, 2021; Qiu et al.,

2024; Wilson et al., 2014; Zhou et al., 2021). The OFC is thought to represent a subject's location within a map (Bradfield & Hart, 2020; Park et al., 2020, Wilson et al., 2014) and is particularly receptive to goal-relevant information (Wikenheiser et al., 2021). Rodent studies indicate that the rat OFC can construct complex mental maps of observable and non-observable stimuli, aiding in processes of prediction and decision making (Tolman, 1948). In this vein, our research attempts to better understand the role of the OFC in the initial stages of creating and manipulating cognitive maps of an abstract auditory space. Specifically, we are interested in how OFC manipulation hinders rats' ability to learn the auditory stimuli as interdependent, and whether this manifests in alternative, less efficient learning strategies.

In addition to cognitive mapping, the OFC is implicated in relevant processes such as prediction, generalization, encoding relations between variables and events, problem solving, learning set formation, economic decision making, and credit assignment (Gardner & Schoenbaum, 2021; Schuck et al., 2016; Zhou et al., 2021). While researchers generally agree that the OFC plays a key role in these functions, questions remain regarding the exact nature of this role (Gardner & Schoenbaum, 2021; Wilson et al., 2014). For instance, there is some ambiguity regarding how the OFC contributes to learning and prediction-based decision making (Bradfield & Hart, 2020; Gardner & Schoenbaum, 2021; Wilson et al., 2014). While the predominant theories may not account for all causal findings, the mixed nature of this data suggests that the OFC plays a highly nuanced role in cognitive mapping. Researchers propose that the OFC may be required for the creation of new cognitive maps; however, once a model has been consolidated into long term memory, the necessity of the OFC is diminished. It is believed that the OFC is primarily responsible for providing the current task model, which is then offloaded to other brain regions in reinforcement learning (Gardner & Schoenbaum, 2021).

Cognitive map theory suggests that the OFC combines long term memories about previous experiences with perceptual information from across modalities to provide better predictive information regarding the current scenario. While these mental models are likely also encoded in other brain regions, the OFC is distinguished by its ability to disambiguate sensory similarities from conceptual differences. The OFC integrates external, perceptually available information with knowledge stored in long-term memory to create a rich representation of a given state or task (Gardner & Schoenbaum, 2021; Schuck et al., 2016; Wilson et al., 2014).

The relationship between the OFC and hippocampus has been well-studied and appears to be important for storing task information when it is not explicitly signaled by the environment. Both the OFC and hippocampus are implicated in the encoding of cognitive maps, with some research proposing that these brain regions interact to perform this function (Mizrak et al., 2021; Wikenheiser & Schoenbaum, 2016; Wikenheiser et al., 2021). Specifically, the interaction between these regions is thought to play a role in the maintenance of mental maps in both humans and rodents. Research in the latter population suggests that manipulating the OFC or hippocampus can impact the subject's effectiveness in decision making tasks (Behrens et al., 2018). Additionally, both regions are associated with model-based inferencing (Park et al., 2020). The hippocampal formation is also implicated in processes of spatial encoding (Wikenheiser et al., 2021) and integrating of spatial and temporal information (Park et al., 2020). Further, the hippocampal-entorhinal circuit is frequently cited in literature as instrumental to spatial navigation processes (Aronov, Nevers, & Tank, 2017; Whittington et al., 2020). According to research on the navigation of 2-dimensional maps, neural activity in rodents' hippocampal-entorhinal circuit reflects the topography of an abstract paradigm (Aronov & Tank, 2014; Behrens et al., 2018). These brain regions are therefore relevant to integral learning, as they are

implicated in the holistic processing of 2 abstract stimulus dimensions that converge to form a space.

It is likely that multiple brain regions interact to create, maintain, and utilize cognitive maps (Gardner & Schoenbaum, 2021; Zhou et al., 2021). For instance, the ventral prefrontal cortex is largely responsible for encoding physical or abstract location in the map, which can be generalized across similar tasks. This implies the encoding of abstract structural knowledge within this brain region (Behrens et al., 2018), a fundamental step in the formation of cognitive maps. While it is necessary to contextualize the role of the OFC within the greater network of brain regions involved in creating maps, research suggests that the OFC plays a unique role in this process. Correlational data supports the theory that the OFC plays a primary role in extracting structural information from previous maps to create new ones (Zhou et al., 2021). It is also proposed that the OFC enables subjects to maintain a sense of their own location (literally or abstractly) within the cognitive map (Gardner & Schoenbaum, 2021).

While the extent of the deficits may vary by case (Wilson et al., 2014), most data suggests that OFC damage causes appreciable cognitive impairment. For instance, animals with OFC lesions lack the ability to integrate external sensory information with internal knowledge (Wilson et al., 2014). In alternation tasks, monkeys with OFC lesions showed considerable deficits in their ability to choose a rewarded stimulus between 2 alternatives. While the control monkeys excelled at the task, lesioned monkeys performed at chance. These monkeys also struggled with extinction tasks, leading to delays in extinction and a lack of spontaneous recovery. Lesioned subjects performed similarly poorly on devaluation tasks (Wilson et al., 2014).

Specialized Cells

Although Tolman's theory of a cognitive map is based on behavioural data, contemporary studies have revealed neural correlates at the cellular level. Neural activity in regions such as the hippocampus and entorhinal cortex can mirror spatial navigation in the external environment (Behrens et al., 2018). Specialized cells, such as grid cells, place cells, and band cells, help with spatial navigation and other functions related to cognitive mapping. Such functions include inferential reasoning, imagination, memory, social cognition and theory of mind, and application of previously learned information to novel situations (Behrens et al., 2018; Constantinescu et al., 2016).

Grid cells, most notably located in the entorhinal cortex, are associated with memory, navigation, and measuring distance between 2 locations (Constantinescu et al., 2016; Park et al., 2020). These cells are aligned on a triangular grid and exhibit hexagonal periodicity in their firing patterns, which is subject to variation across sensory fields (Bao et al., 2019; Behrens et al., 2018; Constantinescu et al., 2016; Park et al., 2020). Grid cells generally share a common grid-axis angle within individuals, and are important for encoding relational information about space (Bao et al., 2019). Grid cell activity can be measured during spatial navigation tasks in parts of the medial frontal cortex, medial parietal cortex, and lateral temporal cortex.

Research in olfaction suggests that grid cells help rodents orient themselves within an abstract odor space (Bao et al., 2019). In this case, cellular activity reflects changes in odor intensity as opposed to Euclidean distance (Bao et al., 2019). While the hippocampal and entorhinal regions are associated with grid-like patterns in neuronal activity, grid-like firing observed in the OFC is comparatively weak and infrequent (Wikenheiser et al., 2021).

Interestingly, neural recordings reveal the existence of value-based schemas in the OFC, which

differ from the context-based schemas observed in the hippocampal formation (McKenzie et al., 2016).

This neural data further highlights the complexity with which subjects can map sensory information. Individuals across species exhibit the ability to encode models of both physical and abstract landscapes, with the OFC playing a central role in these processes. The current experiment seeks to better understand this role by investigating how the OFC facilitates integral learning of an abstract map. Due its implication in functions such as relational encoding (Gardner & Schoenbaum, 2021; Zhou et al., 2021), we hypothesize that the OFC is vital to creating integral representations of a 2-dimensional space. We therefore predict that OFC inactivation in the current experiment will hinder learning of compound stimuli and result in lower prediction accuracy.

Methods

Subjects

The initial subject pool consisted of 24 outbred Long Evans rats (12 male and 12 female), from animal provider Envigo (Indianapolis, IN, USA). Although all 24 rats underwent surgery, only 20 rats (11 male and 9 female) survived the post-surgery period. Rats were approximately 6-8 weeks old at the time of acquisition. At acquisition, female rats weighed approximately 250-300g, and male rats weighed approximately 300-350 g. Rats were housed in pairs in transparent plastic boxes (44.5 cm x 25.8 cm x 21.7 cm) with a metal cage top and a combination of paper, sani-chip, and corn-cob bedding. Each box also contained a plastic rectangular tunnel and a nylon bone hanging from the metal rungs. Rats underwent a reverse 12-hour light-dark cycle, so precautions were taken to minimize the amount of fluorescent light exposure during daytime. Rats were fed Laboratory Rodent Diet, a standard rat chow sourced from LabDiet (St. Louis,

MO, USA). Food was placed on top of the cage's metal rungs and regularly replenished. Leading up to the experiment, rats were handled several times a week to promote social health and comfort with the experimenter. Rats were placed on water restriction before the experiment to ensure they were motivated to seek saccharin rewards. This process took place in increments over several days. They received 30 minutes of water access daily for the duration of the experiment, which was provided after the conclusion of both sets of training sessions (around 6pm). When they were not undergoing daily conditioning, rats were kept in the Animal Care Facilities at Concordia University.

Surgical Procedure and Apparatus

All 24 rats underwent stereotaxic surgery in which an adeno-associated viral vector (AAV) was infused bilaterally into the OFC. Initially, half of the rats received an infusion of the experimental AAV8- CaMKIIa-hM4Di-mCherry, and half of the rats received an infusion of the control AAV8-CaMKIIa-mCherry; however, after attrition, the number of experimental and control rats were reduced to 11 and 9 respectively. In the experimental group, rats received an AAV containing AAV8- CaMKIIa-hM4Di-mCherry, which is a designer receptor exclusively activated by a designer drug (DREADD). When combined with certain designer drugs, the virus contained within the DREADD produces a temporary inhibitory effect that is localized to the brain region in which it was infused. The effects of hM4Di are latent in the absence of the drug, as it is the interaction between the drug and the receptor that produces neural inhibition. When the AAV does not contain a DREADD, the mCherry protein is expressed. mCherry, a fluorescent marker, should not produce an inhibitory effect in any context and is therefore used as a control.

To begin surgery, the rat was anesthetized in an induction chamber using isoflurane gas at a concentration of 4-4.5%, depending on body weight. The rat's head was shaved prior to

placement in the stereotax (Kopf Instruments, Tujunga, CA, USA). The rat's head placement was secured using ear bars and a bite bar. To maintain body temperature, the rat was placed on a heating pad for the duration of surgery. Isoflurane was administered continuously through a nose cone that was secured by parafilm. A cotton-tip applicator was used to gently apply eye lubricant. Over the course of the first 20-30 minutes of surgery, the concentration of isoflurane was incrementally lowered to 1.5% for maintenance. Effectiveness of the anesthetic was checked periodically by pinching the rat's toe to ensure a lack of responsiveness.

The rat's scalp was disinfected using an alternation between 70% isopropyl alcohol and iodine. Prior to incision, a 10% dilution of the nonsteroidal anti-inflammatory drug Rimadyl was injected subcutaneously at 1 mg/kg of the rat's body weight. Approximately 0.15 mL of the local anesthetic lidocaine was injected into the scalp. The Rimadyl and lidocaine used in this experiment were sourced from CDMV (Saint-Hyacinthe, QC, Canada). A sterile scalpel was then used to draw an incision from the anterior to the posterior of the scalp, followed by the removal of fascia using a surgical scraper. Hemostatic forceps were used to pull and secure the rat's skin away from the skull. Sterile gauze and cotton-tip applicators were used to blot excessive bleeding. In some cases, a cautery tool was used to singe blood vessels. Once the bone was sufficiently clear of fascia, a microscope was used to locate bregma and lamda on the skull. A stereotax arm was used to measure the height of these coordinates. If the skull was not level, the height of the nose cone was adjusted accordingly.

Once the skull had been levelled, a drill was attached to the stereotax arm and zeroed on bregma. To access the OFC, bilateral holes were drilled on either side of bregma at the coordinates 2.9 mm A/P and 3.1 mm M/L in rats weighing under 300 g, and 3.0 mm A/P and 3.2 mm M/L in rats weighing over 300 g. Drilling stopped once dura had been broken and a small

amount of cerebrospinal fluid was released. Using 26-gauge stainless steel cannulae from McMaster-Carr (Elmhurst, IL, USA), 2 1 ul syringes from Hamilton Co. (Reno, NV, USA) were partially loaded with deionized water. A small air bubble was created by gently sliding the plunger back. The syringe was once again loaded with deionized water before being loaded with the AAV. The AAVs were obtained from the Neurophotonics Centre at University of Laval (Quebec City, QC, Canada). Each vial contained 5 uL of AAV, stored in a -80°C freezer until use. Once the syringe was loaded, it could be used for up to three surgeries within a day.

The syringes were secured into a syringe pump from Hamilton Co. The cannulae were carefully clamped to each stereotax arm, which were then zeroed on bregma and placed in the coordinates corresponding to the OFC. Over the course of approximately 5 minutes, the cannulae were gradually lowered to a depth of 5.3 mm D/V in rats under 300 g and 5.5 mm D/V in rats over 300 g. 1.0 uL of AAV was infused at a rate of 0.1 uL/minute, followed by a ~5-minute recovery period. Once the cannulae had been gradually removed, bone wax was applied with a surgical scraper to seal the holes in the skull. The forceps securing the skin flaps were removed, and the incision was closed using a reflex clip applicator. The surgical area was disinfected using iodine. To prevent dehydration, approximately 5 mL of saline was injected subcutaneously prior to the cessation of anesthesia. The rat was left on the heating pad and monitored until the anesthetic wore off.

Each rat received the same injection of Rimadyl (10% dilution in saline, injected subcutaneously at 1 mg/kg of body weight) for three days following surgery. Approximately 2 weeks after surgery, the rat was anesthetized and remaining reflex clips were removed. Since DREADD expression requires a minimum of 2-3 weeks (Smith et al., 2016), the behavioural experiment began 4 weeks post-operation.

Behavioural Apparatus

Behavioural training sessions took place in 30.5 cm x 31.8 cm x 29.2 cm conditioning boxes (Med Associates Inc., St. Albans, VT, USA). The sides of the boxes were comprised of stainless-steel panels, with a food port (ENV-200R3AM) and a speaker (Adafruit Industries LLC, PN: 1669) on the right wall. The back walls, ceilings, and doors of the boxes were comprised of plexiglass. The floors consisted of stainless-steel bars, with a removable stainless-steel tray underneath. The tray was washed with water and replaced daily. 2 Raspberry Pis (Raspberry Pi Foundation, Cambridge, UK) were mounted on the outside of each conditioning box, connecting the box to a computer. The experimental procedure was run on Raspberry Pis using custom-written Python code. 1 Raspberry Pi was connected to the conditioning box, whereas the other was connected to a NoIR v2 camera (Adafruit Industries) for video data collection.

On alternating days, 60 mL syringes were loaded with saccharin solution (0.55 g of saccharin diluted in 1 L of water) and hooked into an automated pump (PHM-100, 3.3 RPM) outside each conditioning box. Syringes were clamped with a butterfly clip to prevent slippage during the experiment. The pumps delivered ~80 ul of saccharin solution through plastic tubing connected to the magazine each time a rewarded cue was played, dispensing a total of ~3.9 mL of solution per training session. The saccharin was replaced with a fresh solution every other day. Syringes were thoroughly rinsed with each replacement, and the line was cleaned by running water through the tubing connecting the syringes to the food port.

The auditory cue sequence and the reward dispensation were automated via customized code. The auditory cues were played through the speakers in the conditioning box. Anticipatory responding was logged via a laser-beam in each food port. Every time the rat poked its nose into

the port in search of food, the laser-beam break was automatically logged as an instance of reward anticipation. The data suggested that rats took approximately 45 seconds to consume the saccharine reward, as they remained in the food port for ~15 cues following a reward (Figure 1). Nose pokes were therefore not logged for the 15 cues during and after the reward. To prevent auditory interference between the boxes, each conditioning chamber was placed in a soundproof box with a fan. The video cameras, which were aligned with the middle of the conditioning box, were magnetically mounted on the ceiling of each soundproof box. Experiment footage was used only to supplement data analysis, which was based on the number of laser-beam breaks recorded per session.

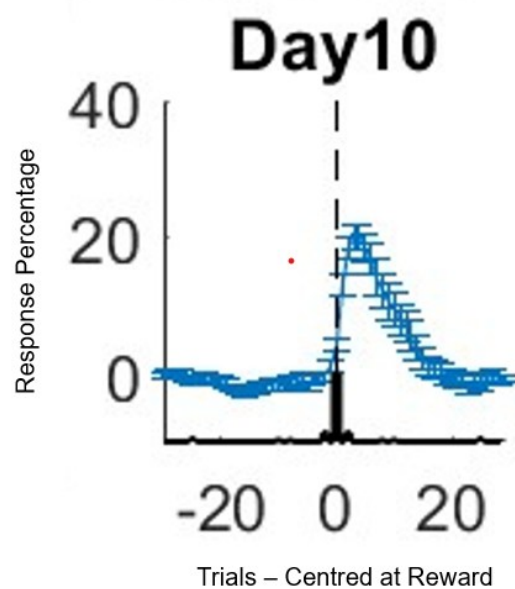


Figure 1: Graph depicting response percentage on Day 10 of the current experiment. The dashed line (0) represents the rewarded cue. The values to the left of the line represent the cues preceding the reward, while the values to the right represent the cues following the reward. The blue line depicts aggregate response percentage across all rats, which peaks in the cues immediately following a reward and reaches baseline within 15 cues.

Behavioural Paradigm

This experiment tests integral learning using a paradigm referred to as the cue map. The cue map, which is an abstract, 2-dimensional matrix, consists of 144 compound auditory stimuli. Each cue represents a pixel on the matrix. Cues are comprised of 2 auditory stimulus dimensions, a clicker frequency and a tone frequency, which are played in tandem for a total of 3 seconds. The matrix is oriented such that each stimulus dimension varies across either the x-axis or the y-axis. There are 12 distinct tone frequencies (ranging from 795 hertz to 14,248 hertz) and 12 distinct clicker frequencies (ranging from 2.00 hertz to 35.84 hertz). Each cue increases by a factor of 1.3 units per cue. The orientation of stimulus dimensions on the matrix is counterbalanced across rats, with a total of 4 potential combinations.

The transition structure between these pixels is determined by the order in which the auditory cues are played. Although the auditory space is entirely 2-dimensional, the progression of cues is designed to mimic allowed movement through physical space. Specifically, each cue must succeed an adjacent cue. This means that either the tone or the clicker frequency increases by 1 pixel at a time; however, the trajectory of the rat's so-called movement through the space is randomized within these constraints, yielding a semi-randomized transition structure referred to as the 'random walk trajectory' (Figure 2A). There is no correlation between the cue map and the topography of the rat's physical environment. The rat's location within the conditioning chamber is therefore irrelevant to the predetermined sequence of auditory stimuli.

To motivate and test learning, 2 of these compound auditory cues were paired with a reward. When these cues were played, rats received saccharin solution through a magazine. The cues paired with rewards were deemed 'reward zones' (RZs). The RZs were diagonally symmetrical, located at the (3,3) and (10,10) coordinates. The complementary cues, which were

located at the (3,10) and (10,3) coordinates, were deemed ‘complementary zones’ (CZs) (Figure 2B). The CZs were not rewarded, despite sharing one coordinate in common with each reward zone. This means that each CZ shared a clicker frequency in common with one RZ and a tone frequency in common with the other. CZs were flagged as an area of interest, as high responding at a CZ despite distance from rewarded locations is indicative of elemental generalization across stimulus dimensions. Over the course of the initial training period (16 days), control rats were expected to learn a paired association and show anticipatory responding (measured by nose-pokes in the food port) on approach to RZs. Anticipatory responding was expected to decrease as the distance from RZs increased (Figure 2C).

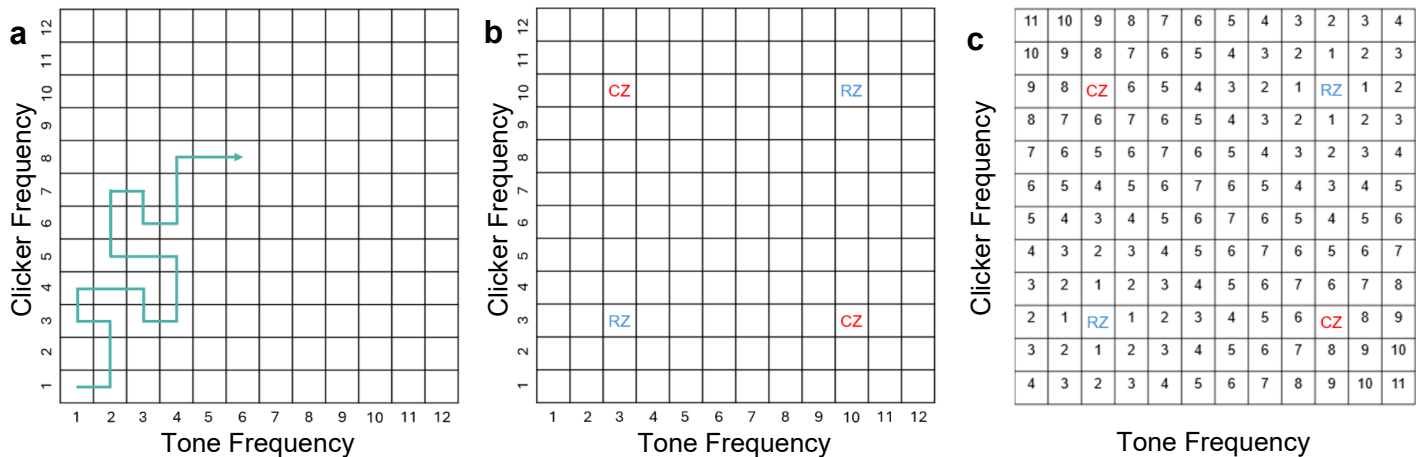


Figure 2: Diagrams of the abstract matrix (cue map) used in the current experiment. **a** Hypothetical segment exemplifying a ‘random walk’ trajectory through the auditory space. The teal line represents the sequence in which the cues are played. Each square symbolizes a different compound auditory stimulus, comprised of the combination of a tone frequency and a clicker frequency. To allow rats to create cognitive maps of the task space, the transition structure of auditory cues within the matrix is designed to mimic physical movement through a space. This means that each cue can only increase by a single pixel at a time, either along the tone frequency axis or the clicker frequency axis. Cue progression is randomized as much as possible within these constraints. In this example, tone frequency is on the x-axis and clicker frequency is on the y-axis; however, this was counterbalanced across rats, so the orientation of stimulus dimensions was not identical for every rat. **b** Diagram with x- and y-coordinates depicting the location of the 2 reward zones (RZ) and 2 complementary zones (CZ). Each number represents a different tone or clicker frequency (e.g. the (1,1) coordinate would be a combination of tone frequency 1 and clicker frequency 1). In this experiment, the RZs were located at the (3,3) and (10,10) coordinates, whereas the CZs were located at the (3,10) and (10,3) coordinates. **c** Diagram showing distance from the nearest reward zone (measured by number of pixels/cues). In normal rats, responding is expected to decrease as the number increases. These numbers reflect the restrictions of the random walk trajectory, which does not allow for diagonal movement between pixels.

Behavioural Procedure

The first day of the experiment (day 0) was a habituation session in which the rats were familiarized with the conditioning box and magazine. Rats received 24 deliveries of saccharin solution with 2-4-minute variable inter-trial intervals to familiarize them with seeking and consuming the saccharin solution. Experimental groups were counterbalanced across 12 conditioning boxes as well as morning and afternoon runs. Males and females were run in separate boxes to avoid sexual chemosignals across sessions. These cohorts remained consistent throughout the experiment. Rats were always placed in the same conditioning box to avoid environmental confounds. After a session of magazine training, rats were ready to begin their training on the auditory cue map. Each day of cue map training consisted of a 175-minute session in which the rats were placed in their conditioning boxes and exposed to many random walks through the auditory space, listening to a total of 3456 cues.

Phase 1: On days 1-16 of training, rats received an intraperitoneal injection of either saline or Agonist 21 (HelloBio, Princeton, NJ, USA), a designer drug that interacts with the CaMKIIa-hM4Di DREADD to temporarily inhibit neurological function through activation of an inhibitory G-coupled protein receptor. Agonist 21 has a high affinity for the DREADD receptor with little to no non-specific effects at the concentration used (Thompson et al., 2018). Rats were injected 30 minutes before conditioning, allowing sufficient time for the agonist to interact with the hM4Di to produce inhibitory effects in experimental rats. 1 mL syringes with 27-gauge needles were used to inject rats with 1 mg of solution per kg of the rat's weight (e.g. a rat weighing 410 g received a dose of 0.41 mL). Rats in the Agonist 21 conditions were injected with a dilution of 0.6 mg of Agonist 21/mL of saline. An extinction test was conducted on day 17, and rats underwent the full task without reward. Injections were counterbalanced, meaning

that the rats that had previously received Agonist 21 now received a saline injection and vice versa.

A factorial design was used to compare learning between conditions. Group 1 (n=5: 3 male, 2 female) consisted of rats in the AAV8-CaMKIIa-hM4Di-mCherry condition who received daily Agonist 21 injections on days 1-16 and a saline injection on day 17. Due to the interaction between hM4Di and Agonist 21, this group was expected to experience OFC-inactivation during the critical learning period spanning the first 16 days of the experiment, with a drug-free test on day 17 to rule out performative effects of the manipulation. Group 2 (n= 6: 3 male, 3 female) consisted of rats in the AAV8-CaMKIIa-hM4Di-mCherry condition who received daily saline injections on days 1-16 and an Agonist 21 injection on day 17. Due to the interaction between hM4Di and Agonist 21, this group was expected to experience OFC-inactivation only on the first extinction test (day 17). Group 3 (n= 5: 3 male, 2 female) consisted of rats in the AAV8-CaMKIIa-mCherry condition who received daily Agonist 21 injections on days 1-16 and a saline injection on day 17. This group should not experience OFC-inactivation at any point during training. Lastly, group 4 (n= 4: 2 male, 2 female) consisted of rats in the AAV8-CaMKIIa-mCherry condition who received daily saline injections on days 1-16 and an Agonist 21 injection on day 17. These groups were run to control for Agonist 21 and the expression of the AAV8 virus.

Phase 2: The experiment was resumed after a 10-day break between days 17 and 18. Beginning on day 18, rats no longer received daily injections. This allowed for a comparison in post-inactivation learning between the previously OFC-inhibited rats (group 1) and their peers. The second phase was designed to test whether experimental rats would display an uptake in learning during post-inactivation trials, and to analyze both the efficiency and accuracy of later

learning. The behavioural design remained the same, where rats underwent 175 minutes of daily conditioning. A second identical extinction test was performed on day 34, on which injections were resumed. 6 rats (consisting of 2 males and 1 female from group 1, and 2 males and 1 female from group 3) were injected with Agonist 21. The remaining 14 rats (consisting of 1 male and 1 female from group 1, 1 male and 1 female from group 3, and all rats from groups 2 and 4) were injected with saline. Rats were perfused following the experiment. Histology is ongoing.

Statistical Analysis

JASP 0.95.4 (JASP Team, Bow, WA, USA), an open-source statistical analysis software, was used to conduct analyses of variance (ANOVAs) comparing the slope of response percentage between experimental conditions across days. The primary goal of these analyses was to investigate the relationship between OFC inactivation and reliance on separable learning. In this instance, separable learning was operationalized as a failure to show differential responding between the RZs and the CZs. Slopes were estimated through a linear regression ($y = \beta_1x + \beta_0$) of the first 5 data points from each session, thus allowing for comparison in response percentage between locations. In most analyses, response slopes were normalized for each rat by subtracting their daily slope measurements at the complementary zones from their daily slope measurements at the reward zones. In addition, post-hoc ANOVAs were conducted to compare all four groups individually.

Results

The current experiment investigates the role of the OFC in integral learning of stimulus dimensions. The OFC was targeted using an AAV infusion containing either an experimental DREADD (AAV8-CaMKIIa-hM4Di-mCherry) or a control (AAV8-CaMKIIa-mCherry). 11 rats were injected with the experimental AAV while the remaining 9 received the control AAV. Once

the 4-week window required for viral expression had elapsed, rats began training on the behavioural paradigm.

Rats received daily pre-trial intraperitoneal injections for the first 16 days of the experiment. These injections contained either saline or Agonist 21, a designer drug that interacts with hM4Di to produce a temporary, localized neural inactivation. Experimental rats receiving Agonist 21 injections experienced putative OFC inhibition for the duration of each training session (Jendryka et al., 2019). Rats received the same type of injection daily for the first phase of the experiment, until injection type was counterbalanced during the extinction test on day 17. This study followed a factorial design in which injection type was split between the experimental groups. Injections were ceased for the second phase of the experiment, allowing experimental rats to learn the paradigm with restored OFC function. A second extinction test was conducted on day 34, in which rats received the same injections as they did during the initial training period.

To test integral learning, we used a behavioural paradigm which we refer to as the ‘cue map’. The cue map is an abstract matrix comprised of 12 distinct tone frequencies and 12 distinct clicker frequencies, which combine to form 144 compound auditory stimuli. Rats were exposed to daily 175-minute training sessions in which a semi-randomized walk sequence of auditory cues was played (Figure 2A). To test learning via anticipatory responding, 2 of the compounds stimuli were paired with a saccharin reward and thus dubbed reward zones (RZs). The 2 complementary stimulus compounds, which were located opposite to the RZs, were dubbed complementary zones (CZs) (Figure 2B). Each CZ shared an x-coordinate in common with one RZ and a y-coordinate in common with the other; however, despite sharing overlapping dimensions with rewarded cues, CZs were not rewarded. Successful reward prediction therefore hinged on the understanding that these stimulus dimensions were functionally integral and not

independently associated with reward. The distance between pixels is measured as the lowest possible number of cues required to get from one point to another within a random walk, which limits movement between cues to horizontal and vertical transitions. In this experiment, the RZs and CZs were located 7 pixels away from one another (Figure 2C). This means that no fewer than 7 auditory cues could be played between a rewarded cue and a complementary zone cue.

Previous behavioural experiments from this lab suggest that rats ultimately learn to anticipate rewards based on temporal proximity to a RZ (Figure 3). This anticipatory responding diminishes as rats are further removed from the RZ. Prior data has indicated that after one month of cue map training, rats showed significantly higher responding at the RZs than they did at the CZs ($F_{(1,1)} = 17.14$, $p < .001$, partial $\eta^2 = 0.311$). Analysis of variance revealed a significant main effect of distance from RZ on responding ($F_{(1,10)} = 102.258$, $p < .001$, partial $\eta^2 = 0.237$). There was also a significant interaction effect of distance and day on responding ($F_{(1,290)} = 1.539$, $p < .001$, partial $\eta^2 = 0.119$) (Figure 5). This data suggests a negative association between response percentage and distance from the nearest reward zone. Rats exhibited integral learning, as evidenced by diminished responding at the complementary zones (Tables 1 & 2).

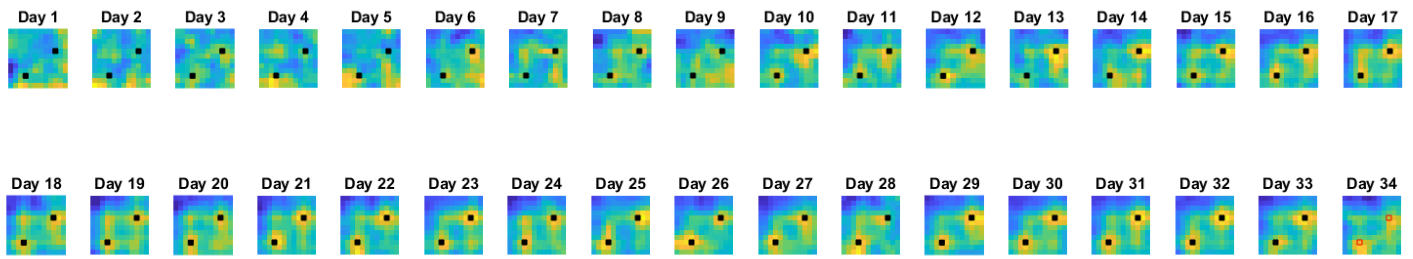


Figure 3: Thermal maps from an earlier experiment representing aggregate response volume (measured by number of nose pokes in the food port) across experimental days. Each pixel on the map represents a different cue in the auditory matrix. The 2 black pixels represent the matrix coordinates of the rewarded cues, referred to as ‘reward zones’. Response volume is gradated by colour and ranges from high responding (yellow) to low responding (blue). These maps depict patterns in responding across days. While rats did not initially show cohesive patterns in responding, their response patterns became increasingly organized over trials. By the last 10 days of the trial, rats were clearly able to identify the RZs and showed consistently high levels of response to proximal cues.

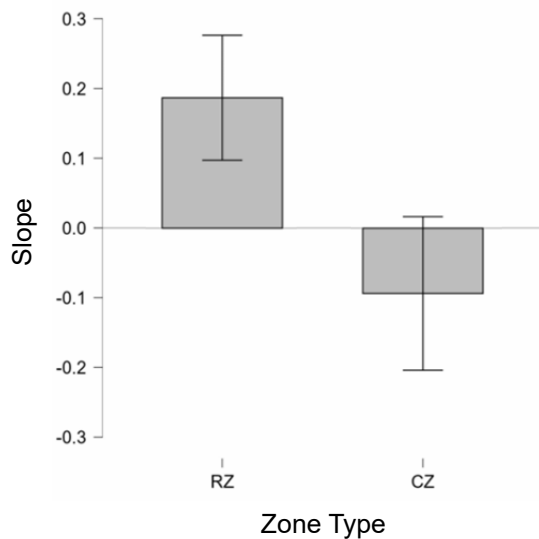


Figure 4: In an earlier experiment from this lab, rats were trained on a ‘random walk’ trajectory of the cue map. This plot compares response slopes between the complementary zones (CZ bar) and reward zones (RZ bar) on day 32. The disparity between the high instances of response at the rewarded locations and low instances of response at the complementary locations suggests that rats effectively learned the stimuli and could distinguish between rewarded cues and nonrewarded cues with overlapping stimulus features.

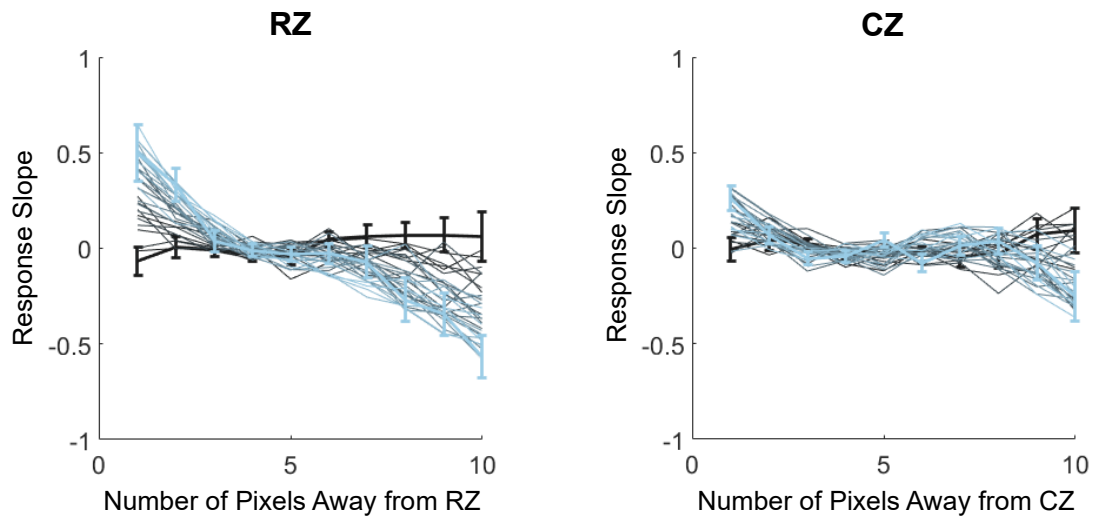


Figure 5: Data from an earlier experiment tracking response volume by distance (pixels away). The line colour gradient is used to depict responding across days, with the black line representing the first trial and the light blue line representing the last trial. The x-axis on the first graph represents pixels (discrete stimulus compounds) away from the reward zones, whereas the x-axis on the second graph represents pixels away from the complementary zones. The lines in the first graph indicate that rats showed higher responding for stimuli closest to the RZs (right panel) in later sessions, with a steeper decrease in responding as distance increased. This pattern is absent for the CZs (left panel).

Once it was established that rats could learn the task, we sought to investigate the specific role of the OFC in the learning process. In the current experiment, we hypothesized that inactivation would inhibit integral learning thus yielding independent and separable learning across stimulus dimensions. We therefore used differentiation between RZs and CZs as the primary metric for integral learning.

To test whether rats showed differential responding across days, we conducted a repeated measures ANOVA comparing response slope between zone types across all training sessions. The fixed factors in this analysis were zone type (RZ versus CZ), AAV type (hM4Di versus mCherry), and injection type (Agonist 21 versus saline). The dependent variable was the slope of

response. There was a significant within-subject interaction between zone type, AAV type, and injection type on slope of response ($F_{(1,1)} = 5.129$, $p = .024$, partial $\eta^2 = 0.008$). There was also a significant between-subject interaction between AAV type and injection type ($F_{(1,1)} = 14.016$, $p < .001$, partial $\eta^2 = 0.022$) (Table 3). There was no significant main effect of either AAV type or injection type between subjects. Repeated measures ANOVAs were then run on data from the first extinction test (day 17) and second extinction test (day 34). The fixed factors were zone type, AAV type, and injection type. The first extinction test yielded no significant main or interaction effects either between or within subjects. This may have occurred because learning was not yet established at this point in the experiment. Analysis of the second extinction test revealed a significant within-subject main effect of zone type on slope ($F_{(1,1)} = 53.560$, $p < .001$, partial $\eta^2 = 0.770$) (Tables 4 & 5), which is consistent with previous data (Figure 6). There was also a significant within-subject interaction effect of zone type and injection type ($F_{(1,1)} = 6.794$, $p = .019$, partial $\eta^2 = 0.298$).

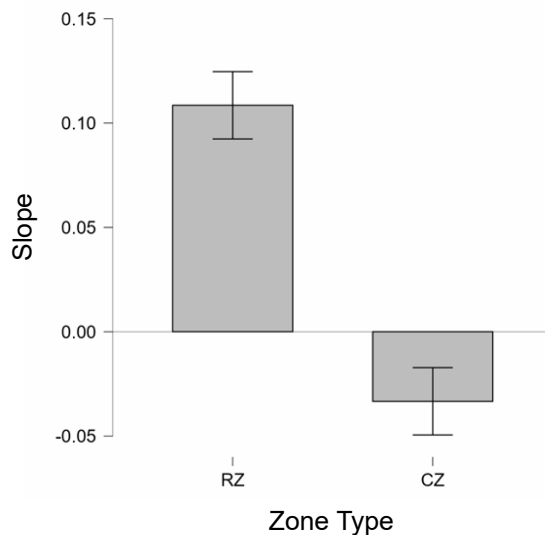
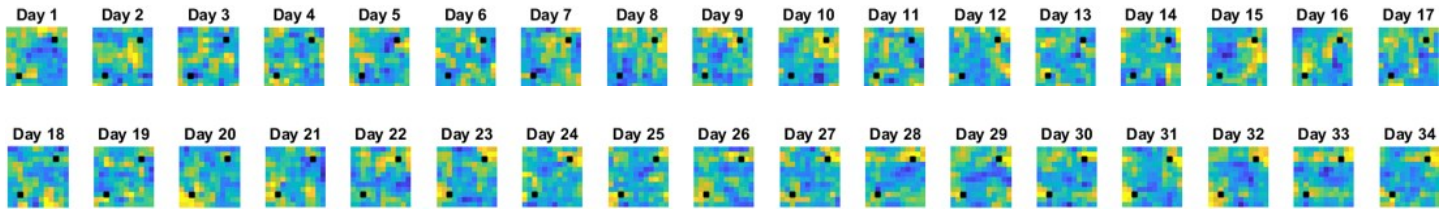


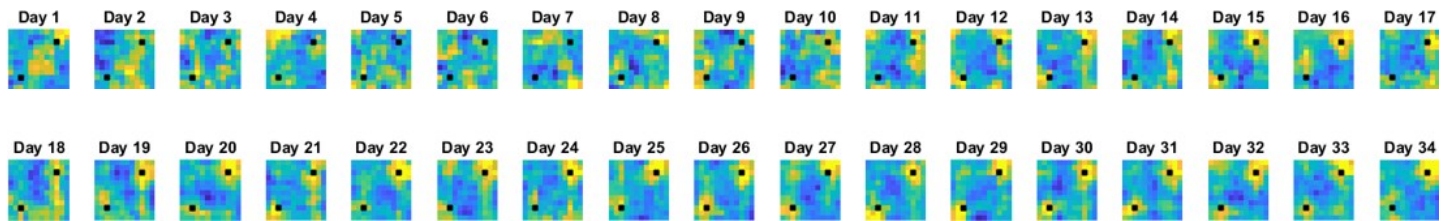
Figure 6: Bar graph from the current experiment depicting aggregate slope of response by zone on the second extinction test (day 34). Rats exhibited differentiation between the RZ and CZ by the final day of the experiment.

We then conducted a 3-way ANOVA across all experimental days except the extinction tests. This test investigated the effects of day, AAV type, and injection type on response slope difference between RZs and CZs. We were particularly interested in the interaction between AAV type and injection type, as OFC inactivation is a product of the interaction between hM4Di and Agonist 21. As hypothesized, the analysis revealed a significant interaction between AAV type and injection type ($F_{(1,1)} = 6.225$, $p = .013$, partial $\eta^2 = 0.012$). The inter-group differences in response volume across all cues can be observed in Figure 7. We also observed significant main effects of day ($F_{(1,31)} = 5.269$, $p < .001$, partial $\eta^2 = 0.242$), AAV type ($F_{(1,1)} = 33.279$, $p < .001$, partial $\eta^2 = 0.061$), and injection type ($F_{(1,1)} = 49.325$, $p < .001$, partial $\eta^2 = 0.088$) (Table 6). While normal rats showed increasing ability to distinguish between RZs and CZs across trials, group 1 rats showed comparable responding between both zone types. This effect was particularly pronounced during the inactivation trials, as slight divergence only occurred during the final days of the experiment (Figure 8A). Normal rats displayed a decrement in responding as the number of pixels away from the RZ increased, with the slope of decrement steepening across days (Figure 9). It should be noted that there was an issue with data collection on day 12 for one rat.

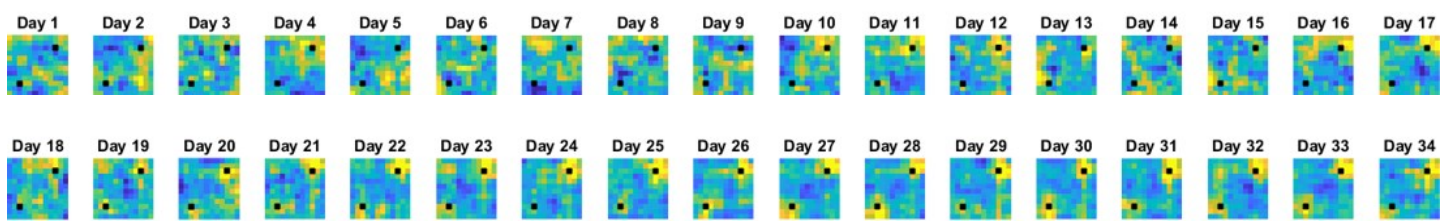
Group 1 (hM4Di-A21)



Group 2 (hM4Di-Sal)



Group 3 (mCher-A21)



Group 4 (mCher-Sal)

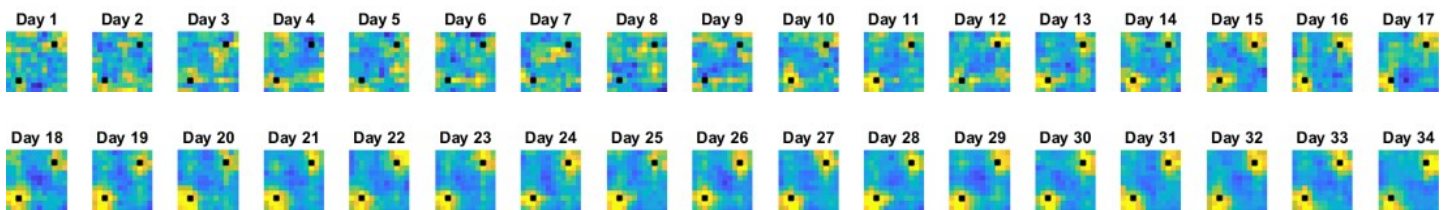


Figure 7: Thermal maps from the current experiment depicting response volume by group. The black pixels represent the RZs. Group 1 rats received an hM4Di infusion and daily injections of Agonist 21 for the first 16 days (phase 1) of the experiment. These rats showed learning impediments during inactivation trials and subsequent delays in uptake. The remaining rats did not undergo OFC-inactivation during phase 1. In comparison to experimental rats, subjects in groups 2-4 exhibited learning through increasingly cohesive anticipatory responding across trials.

We further analyzed inter-group differences through post-hoc testing. The data revealed significant differences in response slope between groups 1 and 2 ($P_{\text{tukey}} = .004$), groups 1 and 4 ($P_{\text{tukey}} < .001$), groups 2 and 4 ($P_{\text{tukey}} < .001$), and groups 3 and 4 ($P_{\text{tukey}} < .001$). No significant difference was found between groups 2 and 3 ($P_{\text{tukey}} = .785$) and groups 1 and 3 ($P_{\text{tukey}} = .091$). Analysis of sex differences across all days revealed a significant main effect of rat sex on slope ($F_{(1,1)} = 9.400$, $p = .002$., partial $\eta^2 = 0.007$), suggesting there may have been an association between sex and cue map learning (Table 7).

Next, we conducted 2 3-way ANOVAs to separately analyze response patterns during each phase. Rats showed signs of learning across the first 16 days of the experiment as evidenced by a main effect of day on RZ slope - CZ slope ($F_{(1,15)} = 3.571$, $p < .001$, partial $\eta^2 = 0.173$). In contrast, analysis of phase 2 revealed no main effect of day on slope ($F_{(1,15)} = 1.012$, $p = .443$, partial $\eta^2 = 0.056$), as control rats reached asymptotic learning in the early stages of the second phase. Unlike the previous analysis of all training days, there was no significant interaction effect between AAV type and injection type in either phase 1 ($F_{(1,1)} = 3.377$, $p = .067$, partial $\eta^2 = 0.013$) or phase 2 ($F_{(1,1)} = 2.933$, $p = .088$., partial $\eta^2 = 0.011$) alone (Figure 8B, Tables 8 & 9). While the drug was not administered during phase 2 of the experiment, the interaction between injection type and AAV type was analyzed to better understand how OFC inactivation during previous trials affected later learning.

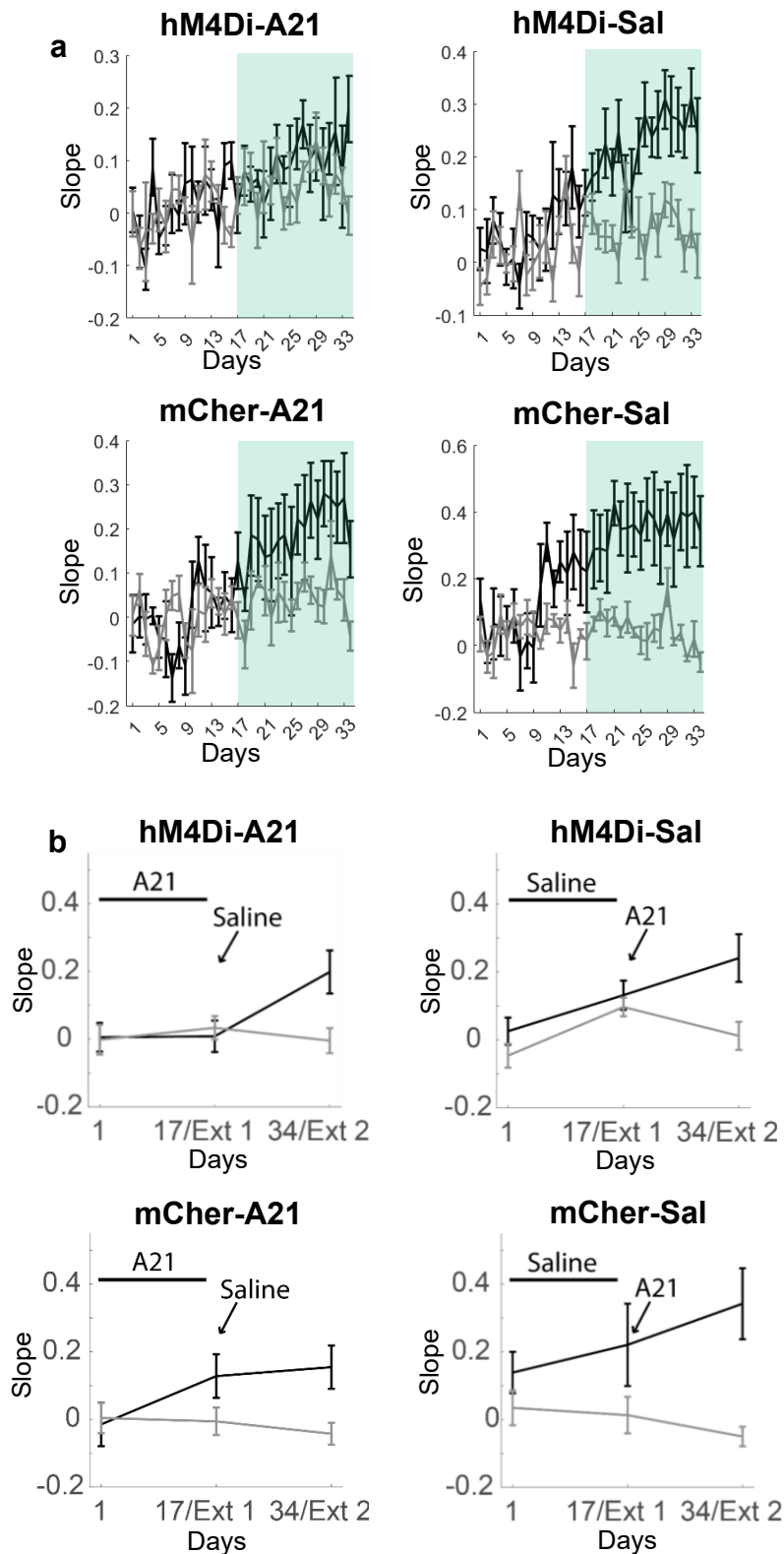


Figure 8: Slopes comparing responding between the reward zones (black lines) and complementary zones (grey lines). **a** Daily slope in both phases with error bars. The green bar is used to indicate post-injection training sessions (phase 2). **b** Linear response slopes during both phases with extinction tests 1 and 2. The injection type administered during the first extinction test is indicated in each graph. This data illustrates differences in responding between the first and second phases of the experiment. The first graph (in the upper left panel) depicts the uptake in learning in experimental rats for inactivation and post-inactivation³³ trials.

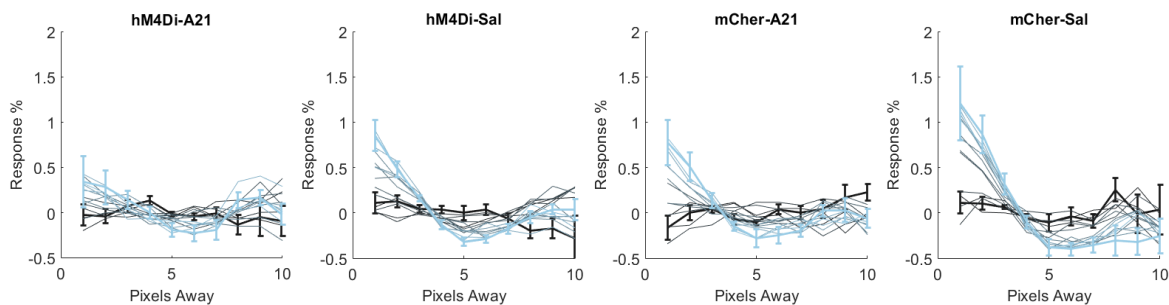


Figure 9: Change in response at reward zones between groups (normalized to standard deviation). Line colour gradient is used to depict responding across days, with the black line representing the first session and the light blue line representing the 16th session. Error bars represent SEM.

Discussion

While the concept of cognitive maps is well-established in neural research, the specific mechanisms underlying this process remain less clear. We argue that in order to create a map, individuals must first learn the integral configurations of stimuli within the environment. In the broader framework of cognitive mapping, the purpose of this experiment was to establish that normal subjects exhibit integral learning of a 2-dimensional auditory task space. Further, we were specifically interested in the role of the OFC in this process. We wanted to investigate the association between OFC-inactivation and separable learning, which was measured by comparing RZ responding to CZ responding. High responding at the CZ suggests separable analysis of stimulus dimensions, in which the rat forms independent associations between certain clicker frequencies/tone frequencies and the reward. The evidence from this study suggests that rats with normal OFC function reached asymptotic learning and were effective in their ability to

predict rewards. Conversely, the experimental group showed delayed learning, even after cessation of injections.

Our analysis suggests that rats with normal OFC function can distinguish between at least 4 states (2 RZs and 2 CZs) in the cue map. It is uncertain whether this represents biconditional discrimination or whether their learning encompasses all possible transition structures within the cue map matrix. Although the granularity of this map is unclear, previous data from this lab suggests that rats presented with a similar task can learn to discriminate between at least 9 states. To our knowledge, it has not been tested whether the OFC is required for the learning of a biconditional discrimination, a finding that would not be surprising given our results.

Most rats exhibited learning over the course of the task. When comparing responding at RZs to CZs on the first extinction test, we found no significant main or interaction effects of zone type, AAV type, or injection type on slope of response. However, we observed a significant effect of zone type on the second extinction test, suggesting that differentiation occurred during the second phase. While we found a main effect of day on response slope during the first phase of the experiment, control rats required slightly longer than 16 days to reach asymptote, which could account for the lack of interaction observed between AAV type and injection type during this period. Although previous data suggests that rats predict rewards with relative accuracy after 12-16 days of cue map training, control rats in the current experiment only reached asymptotic learning around day 20. Nevertheless, control rats showed clear discrimination between RZs and CZs for the majority of phase 2.

We observed a decrease in responding as control rats' position in the abstract map moved further away from the RZs. Since each CZ was at minimum 7 cues away from a reward zone, rats with normal OFC function should learn that CZ cues are not predictive of imminent reward.

The high CZ responding observed in experimental subjects suggests stimulus-response learning, where rats developed associations between the reward and independent dimensions. These rats showed generalization across dimensions that were part of a rewarded configuration, leading to anticipatory responding in the absence of an imminent reward. Conversely, the clear differentiation between RZs and CZs observed in control rats indicates integral learning that is consistent with a map-like understanding of the space. These patterns in responding suggest that rats are using configural representations by assimilating multiple dimensions into a coherent context from which they can infer future outcomes (Goldfarb et al., 2021).

It is unclear why there was a significant main effect of injection type on response slope across all experimental days, as neither the injection nor the AAV should independently impact cognitive function. It is also unclear why there was a significant interaction between zone type and injection type on the second extinction test. While unlikely, the possibility that Agonist 21 alone impacted cognitive function cannot be ruled out. It is also possible that these effects were observed due to the low sample size of each group. Consequent variance may also be responsible for some of the differences observed between control groups, which should theoretically yield consistent results. This study should be repeated with a higher number of subjects to ensure the results are not impacted by potential variance issues.

Our findings are consistent with literature suggesting that the OFC is instrumental to determining the initial orientation within a task space and making predictions about future positions (Bradfield & Hart, 2020). The findings also align with chemogenetic data from Peterson et al. (2024) suggesting that OFC-inactivation impairs rats' performance on context-dependent discrimination tasks, retrieval from long term memory, and the formation of new associations and schema. Specifically, they found that OFC- and dorsal hippocampus-

inactivation does not impact direct cue-reward associations, but rather inhibits the ability to integrate newly learned associations with previous contextual representations.

The OFC likely plays a key role in determining initial position within a cognitive map; however, research suggests that the OFC may not be critical for drawing on previously established internal models (Gardner & Schoenbaum, 2021; Wilson et al., 2014). While the OFC-inactivated rats in our study exhibited a gradual uptake in learning during post-inactivation trials, their learning trajectory was significantly blunted by interference during the critical learning period. Their responding at the RZs and CZs only began to diverge towards the end of the second phase.

Many researchers argue that integrality exists on a scale, and that this concept can be ambiguous and controversial in definition (Burns & Shepp, 1988; Cheng & Pachella, 1984; Pomerantz & Sager, 1975; Shepard, 1991; Wood, 1974). This study is designed such that accurate reward prediction relies on integral learning of the stimulus dimensions, allowing rats to differentiate between rewarded and unrewarded cues. It is important to note that while these cues are played in tandem, they are sonically distinct enough to be perceived separably. The distinction between integral and separable stimuli is sometimes unclear, and the potential for factorial analysis of stimulus dimensions does not necessarily preclude integral learning (Blunden et al., 2015; Cheng & Pachella, 1984). Each compound cue in this paradigm represents a single state. Although the tone and clicker frequencies may be analyzed independently, they become functionally integral once contextualized within the cue map. Rats that understand these cues as integral can predict rewards with greater accuracy, producing fewer false positives and false negatives.

This theory aligns with previous research suggesting that both the context of the paradigm and the subject's demographics may influence perception of stimulus dimensions. For instance, there is evidence that subjects may learn to process separable stimuli as integral over time (Blunden et al., 2015). Some developmental studies claim there is an association between youth and integral processing, where dimensions considered separable by adults are often perceived as integral by children (Smith & Kemler, 1978). Interestingly, Cook and Odom (1992) challenge the basis for this assumption, as their research finds no effect of age on dimensional selectivity. Their argument nevertheless highlights the role of context on perceptual processing. Specifically, Cook and Odom argue that since prior data is based on vague free classification tasks, it fails to consider the probability that children are classifying according to similarity on one of the dimensions. This highlights the influence of the experimental paradigm on the ways subjects process, or at the very least respond to, stimuli. It is likely that the stimulus's inherent characteristics are only partly responsible for determining the way in which the subject responds; therefore, the context of the experiment has some bearing on how the stimulus is learned. While the stimulus dimensions in our experiment are perceptually distinct from one another, they are correlated in the context of the paradigm. Treating each stimulus dimension as separable and independently predictive of reward yields incorrect predictions, whereas integral learning of the cues facilitates accuracy.

It is possible that although the clicker and tone frequency are not sonically blended, their synchronicity is conducive to integral learning. In future research, it is worth investigating whether sensory modality itself plays a role in generalization strategy, and whether certain senses are associated with an increased tendency towards integral representations. Much of the early research on stimulus dimensions is based on visual stimuli. However, in 1975, Garner discussed

cross-modality generalization and reviewed evidence of integrality in auditory stimuli. Based on data from Wood, Garner argued that individuals tend to treat the pitch and volume of an auditory stimulus as integral dimensions. This finding was replicated in later data (Grau & Kemler Nelson, 1988; Melara & Marks, 1990), but there is a gap in the literature regarding whether sensory modality itself interacts with stimulus properties to influence the degree of integral learning. While our design investigates audition, future experiments may use cross-modality paradigms to analyze processing differences between senses.

There were several limitations to this study. Foremost, the sample size was small and unbalanced between experimental groups, necessitating replication with a greater subject pool. Although the normalization of response slopes across locations may yield more conservative statistical tests, the analysis could be skewed due to high variance. This study should be repeated so the power is sufficiently high to test for an effect. Without replication, there is insufficient data from which to generalize to a greater population. In addition, there may be a potential confound of DREADD desensitization due to repeated inactivation (Roth, 2016), although this is unlikely as the experimental rats showed consistent deficits over the course of the injection period.

Cognitive mapping may be broadly defined, and it can be difficult to conclusively establish that animals are using cognitive maps in navigating an abstract space. We decided to approach this problem by first establishing that rats can learn the integral representations that are required to create a cognitive map. Previous data from this lab suggests that rats exposed to the cue map learn to predict rewards on approach to a RZ, but do not show the same responding on an orthogonal pass (despite proximity to the RZ). To assess whether these rats create cognitive maps of abstract landscapes, future research is needed to establish a) the granularity of states within the map, and b) understanding of transition structures between these states.

The current study identified integral learning of an abstract matrix via behavioural analyses, but neural recording studies may further reveal the parallels between the encoding of physical and abstract spaces. Neural data from the hippocampal formation suggests analogous firing patterns between spatial and auditory stimuli, which supports the hypothesis that the brain may map auditory dimensions similarly to how it maps the physical environment. Regarding auditory stimuli, Behrens and colleagues (2018) found evidence that place cells localized in the hippocampus fire in response to variation in sound frequency. Further, the interaction between the hippocampus and the OFC may play a unique role in cognitive mapping and should therefore be studied using abstract paradigms. According to complementary learning systems theory, the hippocampus rapidly encodes context-dependent episodic and spatial information, which is instrumental to the formation of relational memory (Peterson et al, 2024; Whittington et al., 2020; Wikenheiser & Schoenbaum, 2016). Via system consolidation process, this information is then consolidated into existing knowledge structures in the neocortex (McClelland, McNaughton, & Lampinen, 2020; McKenzie et al., 2016; Peterson et al., 2024; Tse et al., 2007). If schemas and cognitive maps are already consolidated into long-term memory in the cortex, this may reduce the duration of encoding within the hippocampus going forward. Since the dorsal hippocampus-OFC circuit is implicated in the consolidation of cognitive maps, it may be worth investigating how these interactions support integral learning of an auditory space.

Conclusion

The current study suggests that the OFC is instrumental in integral learning of an abstract matrix in rats, which may ultimately support the creation of a cognitive map. In this task, integral learning allows rats to attend to relevant stimuli, thus facilitating accuracy in their goal-directed behaviour. This is a hallmark of flexible cognition and can serve processes like future thinking,

reward prediction, and decision making. While there is not enough data from this design to infer that rats are necessarily creating cognitive maps, there is evidence of integral learning, which is a foundational step in this process.

References

- Aronov, D., & Tank, D. W. (2014). Engagement of neural circuits underlying 2D spatial navigation in a rodent virtual reality system. *Neuron*, *84*(2), 442-456. <https://doi.org/10.1016/j.neuron.2014.08.042>
- Aronov, D., Nevers, R., & Tank, D. W. (2017). Mapping of a non-spatial dimension by the hippocampal-entorhinal circuit. *Nature*, *543*(7647), 719-722. <https://doi.org/10.1038/nature21692>
- Bao, X., Gjorgieva, E., Shanahan, L. K., Howard, J. D., Kahnt, T., Gottfried, J. A. (2019). Grid-like neural representations support olfactory navigation of a two-dimensional odor space. *Neuron*, *102*(5), 1066-1075. <https://doi.org/10.1016/j.neuron.2019.03.034>.
- Behrens, T. E. J., Muller, T. H., Whittington, J. C. R., Mark, S., Baram, A. B., Stachenfeld, K. L., Kurth-Nelson, Z. (2018). What is a cognitive map? Organizing knowledge for flexible behaviour. *Neuron*, *100*, 490-509. <https://doi.org/10.1016/j.neuron.2018.10.002>
- Blough, D. S. (1975). Steady state data and a quantitative model of operant generalization and discrimination. *Journal of Experimental Psychology: Animal Behavior Processes*, *1*(1), 3-21. <https://doi.org/10.1037//0097-7403.1.1.3>
- Blough, D. S. (1991). Perceptual analysis in pigeon visual search. In G. R. Lockhead & J. R. Pomerantz (Eds.), *The perception of structure: Essays in honor of Wendell R. Garner* (pp. 213-225). American Psychological Association.
- Blunden, A. G., Wang, T., Griffiths, D. W., & Little, D. R. (2015). Logical-rules and the classification of integral dimensions: Individual differences in the processing of arbitrary dimensions. *Frontiers in Psychology*, *5*(1531), 1-24. <https://doi.org/10.3389/fpsyg.2014.01531>
- Bradfield, L. A., & Hart, G. (2020). Rodent medial and lateral orbitofrontal cortices represent unique components of cognitive maps of task space. *Neuroscience and Biobehavioral Reviews*, *108*, 287-294. <https://doi.org/10.1016/j.neubiorev.2019.11.009>
- Burns, D. M. (2016). Garner interference is not solely driven by stimulus uncertainty. *Psychonomic Bulletin & Review*, *23*(6), 1846-1853. <https://doi.org/10.3758/s13423-016-1054-1>
- Burns, B., & Shepp, B. E. (1988). Dimensional interactions and the structure of psychological space: The representation of hue, saturation, and brightness. *Perception & Psychophysics*, *43*(5), 494-507. <https://doi.org/10.3758/BF03207885>
- Cheng, P. W., & Pachella, R. G. (1984). A psychophysical approach to dimensional separability. *Cognitive Psychology*, *16*(3), 279-304. [https://doi.org/10.1016/0010-0285\(84\)90011-2](https://doi.org/10.1016/0010-0285(84)90011-2)

- Constantinescu, A. O., O'Reilly, J. X., & Behrens, T. E. J. (2016). Organizing conceptual knowledge in humans with a gridlike code. *Science*, 352(6292), 1464-1468. <https://doi.org/10.1126/science.aaf0941>
- Cook, G. L., & Odom, R. D. (1992). Perception of multidimensional stimuli: A differential-sensitivity account of cognitive processing and development. *Journal of Experimental Child Psychology*, 54(2), 213-249. [https://psycnet.apa.org/doi/10.1016/0022-0965\(92\)90036-6](https://psycnet.apa.org/doi/10.1016/0022-0965(92)90036-6)
- Gardner, M. P. H., & Schoenbaum, G. (2021). The orbitofrontal cartographer. *Behavioral Neuroscience*, 135(2), 267-276. <https://doi.org/10.1037/bne0000463>
- Garner, W. R., & Felfoldy, G. L. (1970). Integrality of stimulus dimensions in various types of information processing. *Cognitive Psychology*, 1(3), 225-241. [https://doi.org/10.1016/0010-0285\(70\)90016-2](https://doi.org/10.1016/0010-0285(70)90016-2)
- Garner, W. R. (1976). Interaction of stimulus dimensions in concept and choice processes. *Cognitive Psychology*, 8(1), 98-123. [https://doi.org/10.1016/0010-0285\(76\)90006-2](https://doi.org/10.1016/0010-0285(76)90006-2)
- Garner, W. R. (1975). *The processing of information and structure*. Psychology Press.
- Goldfarb, E. V., Blow, T., Dunsmoor, J. E., & Phelps, E. A. (2021). Elemental and configural threat learning bias extinction generalization. *Neurobiology of Learning and Memory*, 180, 1-26. <https://doi.org/10.1016/j.nlm.2021.107405>
- Grau, J. W., & Kemler Nelson, D. G. (1988). The distinction between integral and separable dimensions: Evidence for the integrality of pitch and loudness. *Journal of Experimental Psychology. General*, 117(4), 347-370. <https://doi.org/10.1037//0096-3445.117.4.347>
- Householder, A. S., & Landahl, H. D. (1945). *Mathematical biophysics of the central nervous system*. The Principia Press.
- Kato, J., & Okada, K. (2011). Simplification and shift in cognition of political difference: Applying the geometric modeling to the analysis of semantic similarity judgment. *PloS One*, 6(6), 1-9. <https://doi.org/10.1371/journal.pone.0020693>
- McClelland, J. L., McNaughton, B. L., & Lampinen, A. K. (2020). Integration of new information in memory: New insights from a complementary learning systems perspective. *Philosophical Transactions of the Royal Society B: Biological Sciences*, 375(1799), 1-21. <https://doi.org/10.1098/rstb.2019.0637>
- McKenzie, S., Keene, C. S., Farovik, A., Bladon, J., Place, R., Komorowski, R., & Eichenbaum, H. (2016). Representation of memories in the cortical-hippocampal system: Results from the application of population similarity analyses. *Neurobiology of Learning and Memory*, 134, 178-191. <https://doi.org/10.1016/j.nlm.2015.12.008>

- Melara, R. D., & Marks, L. E. (1990). Processes underlying dimensional interactions: Correspondences between linguistic and nonlinguistic dimensions. *Memory & Cognition*, *18*(5), 477-495. <https://doi.org/10.3758/BF03198481>
- Mızrak, E., Bouffard, N. R., Libby, L. A., Boorman, E. D., & Ranganath, C. (2021). The hippocampus and orbitofrontal cortex jointly represent task structure during memory-guided decision making. *Cell Reports*, *37*(9), 1-10. <https://doi.org/10.1016/j.celrep.2021.110065>
- Niv, Y., Daniel, R., Geana, A., Gershman, S. J., Leong, Y. C., Radulescu, A., & Wilson, R. C. (2015). Reinforcement learning in multidimensional environments relies on attention mechanisms. *The Journal of Neuroscience*, *35*(21), 8145-8157. <https://doi.org/10.1523/JNEUROSCI.2978-14.2015>
- Park, S. A., Miller, D. S., Nili, H., Ranganath, C., & Boorman, E. D. (2020). Map making: Constructing, combining, and inferring on abstract cognitive maps. *Neuron*, *107*(6), 1226-1238. <https://doi.org/10.1016/j.neuron.2020.06.030>
- Pearce, J. M. (1987). A model for stimulus generalization in Pavlovian conditioning. *Psychological Review*, *94*(1), 61-73. <https://doi.org/10.1037/0033-295X.94.1.61>
- Pearce, J. M. (2002). Evaluation and development of a connectionist theory of configural learning. *Animal Learning and Behavior*, *30*(2), 73-95. <https://doi.org/10.3758/BF03192911>
- Peterson, S., Chavira, J., Garcia Arango, J. A., Seamans, D., Cimino, E. D., & Keiflin, R. (2024). Partially dissociable roles of the orbitofrontal cortex and dorsal hippocampus in context-dependent hierarchical associations. *Current Biology*, *34*(23), 5532-5545. <https://doi.org/10.1016/j.cub.2024.10.049>
- Pomerantz, J. R., & Sagerm L. C. (1975). Asymmetric integrality with dimensions of visual pattern. *Perception & Psychophysics*, *18*(6), 460-466. <https://doi.org/10.3758/BF03204121>
- Qiu, Y., Li, H., Liao, J., Chen, K., Wu, X., Liu, B., & Huang, R. (2024). Forming cognitive maps for abstract spaces: The roles of the human hippocampus and orbitofrontal cortex. *Communications Biology*, *7*(1), 1-12. <https://doi.org/10.1038/s42003-024-06214-5>
- Rescorla, R. A., & Wagner, A. R. (1972). A theory of Pavlovian conditioning: Variations in the effectiveness of reinforcement and nonreinforcement. In A. H. Black & W. F. Prokasy (Eds.), *Classical conditioning II: Current theory and research* (pp. 64-99). Appleton-Century-Crofts.
- Riley, D. A., & Brown, M. F. (1991). Representation of multidimensional stimuli in pigeons. In G. R. Lockhead & J. R. Pomerantz (Eds.), *The perception of structure: Essays in honor of Wendell R. Garner* (pp. 227-245). American Psychological Association.

- Roth, B. L. (2016). DREADDs for neuroscientists. *Neuron*, 89, 683-694. <https://doi.org/10.1016/j.neuron.2016.01.040>
- Schuck, N. W., Cai, M. B., Wilson, R. C., & Niv, Y. (2016). Human orbitofrontal cortex represents a cognitive map of state space. *Neuron*, 91(6), 1402-1412. <https://doi.org/10.1016/j.neuron.2016.08.019>
- Shepard, R. N. (1987). Toward a universal law of generalization for psychological science. *Science*, 237(4820), 1317-1323. <https://doi.org/10.1126/science.3629243>
- Shepard, R. N. (1991). Integrality versus separability of stimulus dimensions. In G. R. Lockhead & J. R. Pomerantz (Eds.), *The perception of structure: Essays in honor of Wendell R. Garner* (pp. 53-71). American Psychological Association.
- Smith, L. B., & Kemler, D. G. (1978). Levels of experienced dimensionality in children and adults. *Cognitive Psychology*, 10(4), 502-532. [https://doi.org/10.1016/0010-0285\(78\)90009-9](https://doi.org/10.1016/0010-0285(78)90009-9)
- Smith, K. S., Bucci, D. J., Luikart, B. W., & Mahler, S. V. (2016). DREADDs: Use and application in behavioral neuroscience. *Behavioral Neuroscience*, 130(2), 137-155. <https://doi.org/10.1037/bne0000135>
- Soto, F. A., & Wasserman, E. A. (2010). Integrality/separability of stimulus dimensions and multidimensional generalization in pigeons. *Journal of Experimental Psychology. Animal Behavior Processes*, 36(2), 194-205. <https://doi.org/10.1037/a0016560>
- Soto, F. A., Gershman, S. J., & Niv, Y. (2014). Explaining compound generalization in associative and causal learning through rational principles of dimensional generalization. *Psychological Review*, 121(3), 526-558. <https://doi.org/10.1037/a0037018>
- Thompson, K. J., Khajehali, E., Bradley, S. J., Navarrete, J. S., Huang, X. P., Slocum, S., Jin, J., Liu, J., Xiong, Y., Olsen, R. H. J., Diberto, J. F., Boyt, K. M., Pina, M. M., Pati, D., Molloy, C., Bundgaard, C., Sexton, P. M., Kash, T. L., Krashes, M. J., Christopoulos, A., Roth, B. L., et al. (2018). DREADD Agonist 21 is an effective agonist for muscarinic-based DREADDs in vitro and in vivo. *ACS Pharmacology & Translational Science*, 1(1), 61-72. <https://doi.org/10.1021/acsptsci.8b00012>
- Tolman, E. (1948). Cognitive maps in rats and men. *Psychological Review*, 55(4), 189-208.
- Tse, D., Langston, R. F., Kakeyama, M., Bethus, I., Spooner, P. A., Wood, E. R., Witter, M. P., & Morris, R. G. M. (2007). Schemas and memory consolidation. *Science*, 316(5821), 76-82. <https://doi.org/10.1126/science.1135935>
- Tversky, A., & Gati, I. (1982). Similarity, separability, and the triangle inequality. *Psychological Review*, 89(2), 123-154. <https://doi.org/10.1037/0033-295X.89.2.123>
- Wagemans, J., Feldman, J., Gepshtein, S., Kimchi, R., Pomerantz, J. R., van der Helm, P. A., & van Leeuwen, C. (2012). A century of Gestalt psychology in visual perception II.

- Conceptual and theoretical foundations. *Psychological Bulletin*, 138(6), 1218-1252.
<https://doi.org/10.1037/a0029334>
- Whittington, J. C. R., Muller, T. H., Mark, S., Chen, G., Barry, C., Burgess, N., & Behrens, T. E. J. (2020). The Tolman-Eichenbaum machine: Unifying space and relational memory through generalization in the hippocampal formation. *Cell*, 183(5), 1249-1263.
<https://doi.org/10.1016/j.cell.2020.10.024>
- Wikenheiser, A. M., & Schoenbaum, G. (2016). Over the river, through the woods: Cognitive maps in the hippocampus and orbitofrontal cortex. *Neuroscience*, 17(8), 513-523.
<https://doi.org/10.1038/nrn.2016.56>
- Wikenheiser, A. M., Gardner, M. P. H., Mueller, L. E., & Schoenbaum, G. (2021). Spatial representations in rat orbitofrontal cortex. *The Journal of Neuroscience*, 41(32), 6933-6945. <https://doi.org/10.1523/JNEUROSCI.0830-21.2021>
- Wilson, R. C., Takahashi, Y. K., Schoenbaum, G., & Niv, Y. (2014). Orbitofrontal cortex as a cognitive map of task space. *Neuron*, 81(2), 267-279.
<https://doi.org/10.1016/j.neuron.2013.11.005>
- Wood, C. C. (1974). Parallel processing of auditory and phonetic information in speech discrimination. *Perception & Psychophysics*, 15(3), 501-508.
<https://doi.org/10.3758/BF03199292>
- Zhou, J., Jia, C., Montesinos-Cartagena, M., Gardner, M. P. H., Zong, W., & Schoenbaum, G. (2021). Evolving schema representations in orbitofrontal ensembles during learning. *Nature*, 590(7847), 606-611. <https://doi.org/10.1038/s41586-020-03061-2>
- Zong, W., Zhou, J., Gardner, M. P. H., Zhang, Z., Costa, K. M., & Schoenbaum, G. (2023). Schema cell formation in orbitofrontal cortex is suppressed by hippocampal output. bioRxiv. <https://doi.org/10.1101/2023.05.03.539307>

Appendix

Table 1

Analysis of Variance Comparing Response Slope at RZ and CZ on Day 32

Cases	SS	df	MS	F	Sig.	Partial η^2
Zone Type	0.786	1	0.786	17.14	< .001	0.311
Residuals	1.743	38	0.046			

Table 2

Analysis of Variance Results for Responding by Distance from RZ

Cases	SS	df	MS	F	Sig.	Partial η^2
Distance	134.642	10	13.464	102.258	< .001	0.237
Day	2.393	29	0.083	0.627	.940	0.005
Distance * Day	58.779	290	0.203	1.539	< .001	0.119
Residuals	434.505	3300	0.132			

Table 3

Repeated Measures Analysis of Variance by Zone Type Across All Days

<i>Within Subjects Effects</i>						
Cases	SS	df	MS	F	Sig.	Partial η^2
Zone Type	7.072	1	7.072	180.066	< .001	0.221
Zone Type*	1.086	1	1.086	27.642	< .001	0.042
AAV Type						
Zone Type*	1.627	1	1.627	41.428	< .001	0.061
Injection Type						
Zone Type *	0.201	1	0.201	5.129	.024	0.008
AAV Type *						
Injection Type						
Residuals	24.938	635	0.039			
<i>Between Subjects Effects</i>						
AAV Type	0.092	1	0.092	2.475	.116	0.004
Injection Type	0.118	1	0.118	3.173	.075	0.005
AAV Type *	0.520	1	0.520	14.016	< .001	0.022
Injection Type						
Residuals	23.556	635	0.037			

Table 4*Repeated Measures Analysis of Variance by Zone Type on Day 17*

<i>Within Subjects Effects</i>						
Cases	SS	df	MS	F	Sig.	Partial η^2
Zone Type	0.119	1	0.119	3.722	.072	0.189
Zone Type*	0.076	1	0.076	2.383	.142	0.130
AAV Type						
Zone Type*	0.099	1	0.099	3.089	.098	0.162
Injection Type						
Zone Type *	0.026	1	0.026	0.815	.380	0.048
AAV Type *						
Injection Type						
Residuals	0.511	16	0.032			
<i>Between Subjects Effects</i>						
AAV Type	0.067	1	0.067	2.282	.150	0.125
Injection Type	1.016×10^{-5}	1	1.016×10^{-5}	3.474×10^{-4}	.985	2.171×10^{-5}
AAV Type *	0.018	1	0.018	0.633	.438	0.038
Injection Type						
Residuals	0.468	16	0.029			

Table 5*Repeated Measures Analysis of Variance by Zone Type on Day 34*

<i>Within Subjects Effects</i>						
Cases	SS	df	MS	F	Sig.	Partial η^2
Zone Type	1.645	1	1.645	53.560	< .001	0.770
Zone Type*	0.078	1	0.078	2.542	.130	0.137
AAV Type						
Zone Type*	0.209	1	0.209	6.794	.019	0.298
Injection Type						
Zone Type *	0.025	1	0.025	0.809	.382	0.048
AAV Type *						
Injection Type						
Residuals	0.491	16	0.031			
<i>Between Subjects Effects</i>						
AAV Type	3.973×10^{-4}	1	3.973×10^{-4}	0.031	.863	0.002
Injection Type	3.329×10^{-4}	1	3.329×10^{-4}	0.026	.874	0.002
AAV Type *	1.065×10^{-4}	1	1.065×10^{-4}	0.008	.929	5.176×10^{-4}
Injection Type						
Residuals	0.206	16	0.013			

Table 6*Analysis of Variance Results Across All Trials Except Extinction Tests*

Cases	SS	df	MS	F	Sig.	Partial η^2
Day	10.733	31	0.346	5.269	<.001	0.242
AAV Type	2.187	1	2.187	33.279	< .001	0.061
Injection Type	3.241	1	3.241	49.325	< .001	0.088
Day * AAV Type	2.175	31	0.070	1.068	.371	0.061
Day * Injection Type	2.573	31	0.083	1.263	.159	0.071
AAV Type * Injection Type	0.409	1	0.409	6.225	.013	0.012
Day * AAV Type * Injection Type	1.300	31	0.042	0.638	.937	0.037
Residuals	33.644	512	0.066			

Table 7*Sex Differences Across All Days*

Cases	SS	df	MS	F	Sig.	Partial η^2
Sex	5.118	1	5.118	9.400	.002	0.007
Day	28.49	33	0.863	1.585	.019	0.039
Rat * Day	23.93	33	0.725	1.332	.100	0.033
Residuals	701.3	1288	0.544			

Table 8*Analysis of Variance Results for Days 1-16*

Cases	SS	df	MS	F	Sig.	Partial η^2
Day	2.951	15	0.197	3.571	< .001	0.173
AAV Type	0.189	1	0.189	3.423	.065	0.013
Injection Type	0.235	1	0.235	4.271	.040	0.016
Day * AAV Type	0.953	15	0.064	1.154	.309	0.063
Day * Injection Type	0.964	15	0.064	1.166	.299	0.064
AAV Type * Injection Type	0.186	1	0.186	3.377	.067	0.013
Day * AAV Type * Injection Type	0.715	15	0.048	0.865	.604	0.048
Residuals	14.103	256	0.055			

Table 9*Analysis of Variance Results for Days 18-33*

Cases	<i>SS</i>	<i>df</i>	<i>MS</i>	<i>F</i>	<i>Sig.</i>	<i>Partial η²</i>
Day	1.158	15	0.077	1.012	.443	0.056
AAV Type	2.746	1	2.746	35.972	< .001	0.123
Injection Type	4.248	1	4.248	55.647	< .001	0.179
Day * AAV Type	0.474	15	0.032	0.414	.975	0.024
Day * Injection Type	0.368	15	0.025	0.321	.993	0.018
AAV Type * Injection Type	0.224	1	0.224	2.933	.088	0.011
Day * AAV Type * Injection Type	0.585	15	0.039	0.511	.934	0.029
Residuals	19.541	256	0.076			